

Ocean, atmosphere, and cloud quantity on the surface conditions of tidally-locked habitable zone planets

Adnan Bin Alamgir¹, Andrea Salazar²

¹Dhaka Residential Model College, Dhaka, Bangladesh

²Department of Earth and Planetary Sciences, Harvard University, Cambridge, MA

SUMMARY

The study of tidally-locked planets has become an active field of research in recent years due to their interesting properties and abundance in the universe. As one hemisphere of these planets is always facing a star and the other is covered in perpetual darkness, habitable conditions on such extreme worlds were generally considered impossible. However, recent studies have shown that under specific planetary atmospheric and oceanic conditions, temperatures could stay mild enough for the planet to be habitable. In this paper, we created an energy balance model to determine the atmospheric and surface temperatures of tidally-locked worlds as a function of several planetary factors. We hypothesized that these factors—atmospheric and oceanic heat circulation and clouds—are crucial for habitable conditions to exist on these planets. We then assessed what specific set of values of these factors would make habitable conditions possible. We found that global heat transportation cycles act as a major determining factor on the planetary climate and, therefore, habitability. Apart from being in the habitable zone, Earth-like oceans and atmospheric coverage could also be essential for the habitability of tidally-locked planets, which establishes viable criteria in future searches for extraterrestrial life and livable worlds.

INTRODUCTION

The existence of exoplanets—planets outside the solar system—has long left the realm of fiction and has become quite an important topic in the realm of science. Since the first confirmed discovery of an exoplanet in 1992, more than five thousand exoplanets have been discovered, with almost ten thousand more pending confirmation (1). In only a few decades, exoplanetary science has become one of the most active fields of research in astronomy. A large number of ground and space-based telescopes, such as Kepler and Transiting Exoplanet Survey Satellite (TESS), are scouring the sky in search of these distant worlds (2). With the discovery of exoplanets, the question of whether some of them could host conditions suitable for harboring life has become quite intriguing, as many of these exoplanets have rocky surfaces and orbit in the habitable zone around their host stars (3). The habitable zone (HZ) is defined as the region around a star where liquid water could exist: not too cold that water would freeze, nor too hot that all the surface water would vaporize, marking 273–373 K the habitable temperature range (4). As

life on Earth is very much dependent on the existence of liquid water, exoplanets that may have surface water are exciting candidates in the search for habitable planets (5, 6).

A special type of exoplanet is the tidally-locked planet—planets with equal rotational and orbital periods (7). An orbiting planet that is also rotating around its own axis experiences a differential force due to the tidal force acting on it. This results in a frictional torque that slows down the planet's axial rotation until it equals the orbital rotation, at which point the planet is in a rotational equilibrium (7). This process is called tidal locking, with one side of the planet always facing the star while the other side faces away, similar to the Earth's moon, which is tidally locked to Earth (6). Hence, the planet can be divided into two sides, the dayside and the nightside, with the prime meridian known as the terminator marking the boundary between them (7). As tidal locking attains a state of equilibrium, all orbiting planets slowly tend towards this state.

In the spectral classification of stars, M-type is the category of stars with an effective temperature of 2700–3800 K (8). This cool effective temperature range means that their HZs are much closer to the star in comparison to our solar system, typically between 0.01 and 0.05 astronomical units (AU), putting the HZ inside their tidal lock radius (4, 9). Planets that orbit close to their host star, as planets in the HZ of M-type stars do, are subjected to higher tidal forces and become tidally-locked in the timescale of the star's lifetime (9). M-type stars make up almost 75% of all the stars in our galaxy, which implies that tidally-locked planets are almost certainly abundant throughout the universe (3).

Habitability is a rather broad term, with numerous factors playing a role in determining the ability of a planet to support life. For exoplanets, the condition considered most crucial is liquid surface water (10). While other factors may include atmospheric composition, surface features, and gravitational interactions with other celestial bodies, water remains the most reasonable criterion considering its essentiality for life on Earth (11). While HZ is defined as the region able to support liquid water, for tidally-locked planets, the case is complicated due to their usual 'eyeball state': they tend towards a state where the surface temperature is highest at the sub-stellar point (the equatorial point closest to the star), lowers with increasing latitude in the dayside, and becomes near absolute zero in the nightside (12). This makes global heat circulation processes a crucial factor on tidally-locked planets in regulating planetary temperatures and allowing surface liquid water to exist. Thus, an energy balance model incorporating parameters that quantize planetary heat circulation processes could ascertain surface temperatures more accurately and potentially give us a better estimation of habitability for these planets (Figure 1). Our model makes this estimation considering the roles of three planetary factors—the ocean, atmosphere, and cloud

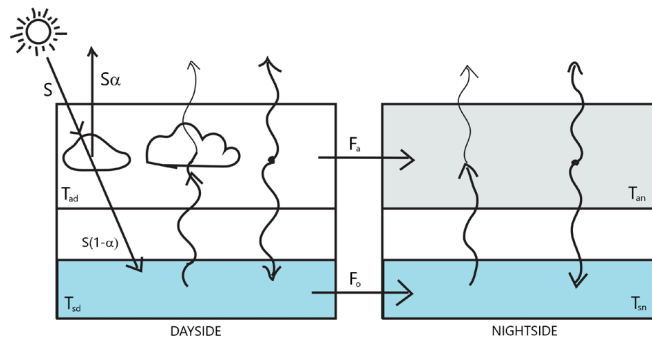


Figure 1: Energy balance box model. The box on the left depicts the dayside and the right depicts the nightside of a tidally-locked planet, with the upper and lower boxes referring to the atmosphere and surface, respectively. This is a one-dimensional energy balance model, as both the atmosphere and the surface only absorb heat they receive from the other system. On tidally-locked planets, atmospheric or ocean heat transport acts as the only source from which the nightside receives any heat energy, and arrows between the boxes depict this energy flow. S , α , T_{sd} , T_{sd} , T_{sn} , T_{sn} , F_a , and F_o respectively denotes stellar flux, albedo, dayside surface temperature, dayside atmospheric temperature, nightside surface temperature, nightside atmospheric temperature, atmospheric heat flux and oceanic heat flux.

content.

On Earth, ocean circulation plays a key role in transporting heat around the planet and maintaining energy equilibrium on a long-term basis (13). On tidally-locked planets, heat currents from the dayside are crucial for the nightside, and oceans can redistribute heat on a global scale efficiently (14). Without a dynamic ocean, the planet would settle into an eyeball state (6, 14). Stable and dynamic atmosphere coverage and greenhouse gases also play a major role in blocking and redistributing heat around the planet so that the nightside atmosphere does not freeze and collapse (15). Lastly, cloud coverage over the planet can significantly increase the planet's reflectivity, or albedo (16). The albedo of a planet refers to the fraction of incident light reflected off the planet and thus limits how much energy is received from the star, making it an important factor in determining planetary temperature and habitability (4).

In this paper, we hypothesized that ocean, atmosphere, and cloud quantity play an essential role in rendering tidally-locked planets habitable. Our model incorporated these planetary parameters to simulate surface temperatures and concluded that these factors tend to drive moderate climates and conditions suitable for surface liquid water. We showcased the structure and effectiveness of this model, along with its implementation using existing planetary dataset.

RESULTS

We developed a planetary temperature model that uses thermal equilibrium conditions on tidally-locked planets to determine their surface and atmospheric temperatures. We introduced three different factors—oceanic heat circulation, atmospheric heat circulation, and cloud quantity—into our energy balance equations. We built the model using variable parameters that best represent these factors – ocean depth for oceanic circulation, atmospheric pressure for atmospheric circulation, and albedo for cloud quantity.

Due to the lack of exoplanet-specific surface and

atmospheric data required to calculate the variable parameters for each exoplanet, such as average ocean depth, atmospheric constituents, and circulation patterns, we instead used an idealized set of constant values derived from the Earth, as these data are readily available, accurate, and a realistic assumption for a terrestrial planet in the HZ (Table 1). In all following analyses, the host star is an M-type star with $T_{star} = 3000$ K.

Model run for an Earth-like planet

Using our model for an Earth-like tidally-locked planet in the HZ, we found that the habitability of such a planet is preserved. The model predicted an exponential decay in surface temperature as distance from the star increases, which correctly converges with the inverse square law for flux (17). Inside the HZ, the median value of the predicted dayside surface temperature is 298.72 K, whereas for the nightside, the predicted value is 238.63 K (Figure 2). These values are quite close to the present-day average temperature of the Earth, which implies that an Earth-like planet should retain its habitable characteristics in a tidally-locked state around an M-type star.

Model run using planetary dataset

We ran our model using the exoplanetary dataset consisting of 17 tidally-locked exoplanets to find their surface temperature values (Tables 2 and 3). We found that in the presence of the variable parameters, the dayside surface temperature lowers substantially, with some planets' temperatures even dropping into the habitable range. In contrast, the temperature on the nightside increases from near-zero values to temperatures above 100 K. The average dayside surface temperature of all 17 planets without considering our planetary parameters was 436 K. When the planetary parameters were included in the model, this became 390 K. In contrast, the average nightside temperature calculated with the parameters included was 270 K, which would be near 0 K without them. For each

Parameters	Symbols	Values
Surface pressure	P_s	10^5 Pa
Relative Humidity dayside	RH_d	0.8
Relative humidity nightside	RH_n	0.6
Ocean depth	z_o	1000 m
Atmospheric Height	z_a	1000 m
Timescale of ocean circulation	γ_o	$(\frac{1}{365})$ days
Timescale of atmospheric circulation	γ_a	$(\frac{1}{30})$ days
Gas constant for atmosphere (N)	R_a	287 Jkg ⁻¹ K ⁻¹
Gas constant for water vapor (H ₂ O)	R_w	461.5 Jkg ⁻¹ K ⁻¹
Emissivity constant	κ	1000
Specific heat of atmosphere	$C_{p,a}$	1000 Jkg ⁻¹ K ⁻¹

Table 1: Idealized parameters used in the planetary energy balance model. The values of these parameters were selected based on their values on Earth. This idealized set of constants for all the planets creates a generalized standard and reduces the possibility of confounding components having an effect.

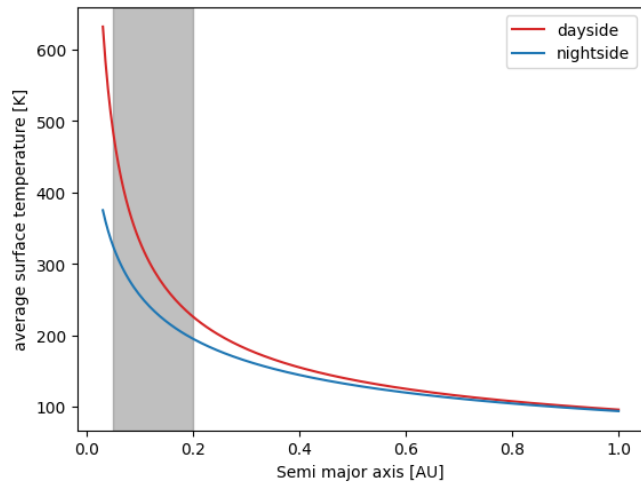


Figure 2: Dayside and nightside surface temperatures against orbital semi major axis. The planet is a tidally-locked planet with Earth-like properties ($\alpha = 0.3$), orbiting a typical M-type star ($T = 3000\text{K}$). The temperatures were calculated from the solution to the energy balance equation using Earth-like parameters. The HZ radius is highlighted (0.05 to 0.2 AU).

of the planets, the average of their respective dayside and nightside temperatures gives an effective planetary average temperature, which falls in the habitable range for a number of planets (Table 3).

Model run for broader analysis

We plotted the surface and atmospheric temperatures with respect to the variable parameters to find any general trend associated with their change. We found that with increasing values of the parameters the differences between the surface and atmospheric temperatures on either side of the planet decrease, resulting in a milder temperature overall (Figures 3-5). For oceanic circulation, the temperatures appeared to flatten out and converge around a central value as ocean depth, and therefore oceanic heat transport, increased (Figure 3). A similar result is observed for atmospheric circulation with increasing surface pressure, but the changes are less drastic than they were for oceanic transportation (Figure 4). Finally, surface and atmospheric temperatures on both sides as well as their difference decrease with increasing albedo, with dayside temperatures showing higher sensitivity to changes in albedo (Figure 5). Overall, we saw that a dynamic atmosphere and ocean with global-scale heat circulation and high cloud coverage move the planet towards a global uniformity in temperature for tidally-locked planets.

DISCUSSION

In our paper, we aimed to assess whether the habitability of tidally-locked exoplanets has a positive correlation with the existence of a dynamic ocean and atmosphere and significant cloud coverage—components that are vital in regulating Earth’s climate systems. Our planetary energy balance model for the surface and atmospheric temperatures of tidally-locked planets considered these components in its calculations and used a habitable temperature range as the criteria for habitability.

With an asymmetric thermal equilibrium condition where one hemisphere of the planet is almost fully cut off from

any heat energy, external means of heat transportation are necessary not only to get the nightside temperature on tidally-locked planets above near absolute zero but also to prevent the dayside from reaching extreme temperatures. According to our results, planetary factors that engender a dynamic heat circulation pattern and the reduction of direct incident sunlight on the dayside surface greatly facilitate the habitability of tidally-locked planets. A dynamic heat-transporting ocean and atmosphere can distribute heat from the dayside to the nightside; thus, an efficient heat transport system can greatly reduce the difference between temperatures in the two hemispheres. Also, planetary cloud coverage—the albedo—can ensure that the temperature in the dayside does not become too high while also being an assistive component to atmospheric circulation (18). Overall, heat energy is better circulated, and temperatures are more optimal. The dayside and nightside surface temperature values our model predicted highlight this contrast (Table 3). Extremely high temperatures on the dayside and near-absolute zero temperatures on the nightside are the characteristics of the planets without any of the planetary factors: ocean circulation, atmospheric circulation, or albedo. After introducing these factors, the surface temperatures shift towards global uniformity. The difference is more noticeable on the nightside, with temperatures rising from near zero to hundreds of Kelvin, with some even having temperatures in the habitable range. This shows the necessity

Planet Name	a_{pl} [10^{-2} AU]	R_{pl} [R_{\oplus}]	M_{pl} [M_{\oplus}]	$T_{eff,star}$ [K]	R_{star} [R_{\odot}]
TRAPPIST-1b	1.154	1.116	1.374	2566	0.12
TRAPPIST-1c	1.521	1.056	1.380	2559	0.12
TRAPPIST-1d	2.144	0.772	0.410	2559	0.12
TRAPPIST-1e	2.817	0.918	0.620	2559	0.12
TRAPPIST-1f	3.710	1.045	0.680	2559	0.12
TRAPPIST-1g	4.683	1.129	1.321	2566	0.12
TRAPPIST-1h	6.189	0.755	0.326	2566	0.12
LP 890-9b	1.875	1.320	13.20	2850	0.16
LP 890-9c	3.984	1.367	25.30	2850	0.16
GJ 1132b	1.530	1.130	1.660	3270	0.21
LHS 1140b	9.570	1.635	6.380	2988	0.21
LHS 1140c	2.734	1.169	1.760	2988	0.21
GJ 1214b	1.411	2.847	6.261	3026	0.22
LHS 1478b	1.848	1.242	2.330	3381	0.25
K2-25b	2.870	3.440	24.50	3207	0.29
L 98-59b	2.191	0.850	0.400	3415	0.30
L 98-59c	3.040	1.385	2.220	3415	0.30
L 98-59d	4.860	1.521	1.940	3415	0.30
TOI-3884b	3.540	6.000	16.50	3269	0.30
GJ 3929b	2.569	1.150	1.210	3369	0.32
TOI-2136b	5.700	2.190	6.370	3342	0.34
K2-146b	2.480	2.250	5.600	3385	0.35
GJ 1252b	0.915	1.180	1.320	3458	0.39
K2-18b	15.91	2.610	8.630	3457	0.44
GJ 436b	3.080	4.100	25.40	3416	0.46
TOI-1685b	1.156	1.459	3.430	3461	0.46
TOI-2285b	13.63	1.740	19.50	3491	0.46

Table 2: Planetary data used from the NASA exoplanet archive (32). The orbital semi-major axis (a_{pl}), planetary radius (R_{pl}), planet’s mass (M_{pl}), stellar effective temperature ($T_{eff,star}$), and stellar radius (R_{star}) data are listed for 17 tidally-locked exoplanets. The temperature values are in the nearest degree Kelvin (K), while the other data are rounded to at most four significant figures for convenience.

Planet name	T_{sd} [K]	T_{sn} [K]	T_{av} [K]	T_{sd}^* [K]	T_{sn}^* [K]
TRAPPIST-1b	491	337	414	542	0
TRAPPIST-1c	422	307	364.5	471	0
TRAPPIST-1d	349	272	310.5	396	0
TRAPPIST-1e	258	196	227	346	0
TRAPPIST-1f	221	178	199.5	254	0
TRAPPIST-1g	195	164	179.5	226	0
TRAPPIST-1h	167	147	157	197	0
LP 890-9b	501	316	408.5	545	0
LP 890-9c	332	251	291.5	374	0
LHS 1140b	222	178	200	255	0
LHS 1140c	492	335	413.5	542	0
K2-18b	329	254	291.5	377	0
K2-25b	525	276	400.5	561	0
L 98-59b	767	449	608	828	0
L 98-59d	503	347	425	556	0
TOI-2136b	485	332	408.5	535	0
TOI-2285b	377	272	324.5	420	0

Table 3: Calculated planetary temperature values for the listed tidally-locked exoplanets. The temperatures were calculated from the developed planetary temperature model. The first three columns (green) were calculated with an idealized planetary heat transport system and an albedo of 0.3, while the next two columns (orange) were without any heat transport and an albedo of 0.15. T_{sd} , T_{sn} denote the dayside and nightside surface temperatures respectively for the former case, while T_{sd}^* , T_{sn}^* denote the same for the latter. T_{av} in the middle column is the average of T_{sd} and T_{sn} . T_{av} values that fall in the habitable range (273K – 373K) are highlighted in blue.

of ocean, atmosphere, and cloud coverage for habitability, which validates our initial hypothesis.

In assessing the role of each individual factor, we saw that all three of them correlate positively with effective global heat distribution. On the surface, ocean circulation is the primary mode of heat transportation. The high specific heat of water means that a deeper ocean will be able to absorb and retain a significant amount of incident heat energy before it circulates into the nightside. With a larger amount of absorbed heat and a higher water current overall, the heat current associated with oceanic energy transportation increases with increasing depth (6). Similarly, a larger air pressure drives the air around the planet's atmosphere much faster, achieving more effective atmospheric heat transport by mixing up the atmospheric heat more evenly while also facilitating the greenhouse effect (19). From our results, we see that at some point the temperatures of the dayside and nightside atmospheres can become nearly equal, thus reaching a dynamic equilibrium as one large system. Larger cloud coverage increases the planetary albedo by covering the planet with a greater reflective component compared to the surface. A lower value of albedo refers to little or no clouds in the atmosphere (when a certain heat convection condition is not satisfied), and a higher value refers to significant clouds in the atmosphere (20). Typically, without clouds, the albedo of planets around M-type stars varies between 0.1 and 0.2 (4). For albedo values larger than this, which implies cloud coverage, the contrast between temperatures on the two sides becomes less prominent. Put together, these factors complement each other, drive the planet towards optimal climate conditions, and have a global effect on planetary climate through controlling heat circulation and received heat energy. For instance, without effective heat

circulation, the planet's nightside atmosphere could condense, which would lead to a complete atmospheric collapse (15). Moreover, extensive cloud coverage can prevent the dayside from reaching extremely high temperatures by blocking excessive starlight.

Some of the exoplanets we considered in our study showed promising prospects for future observations, such as Trappist-1d, Trappist-1e, LP 890-9c, and K2-18b, from their habitable or near habitable range average temperatures (Table 3). The Trappist-1 star system has long been an interesting target for astronomers, as it has seven planets that are all tidally locked to their host star (21). From our results and their characteristics, the planets Trappist-1d and Trappist-1e stand out as having the largest potential for habitability, as the mean of the former's dayside and nightside temperatures fall right in the habitable range (273–373 K) and just below it for the latter (Table 3). This agrees with the results found by Wolf using a 3D climate model, or a general climate model (GCM) (22). The surface temperatures of Trappist-1e may seem too cold to be habitable, but a stable greenhouse effect could make surface liquid water possible at lower latitudes (21). It should be noted that our model determined the average surface temperatures of the dayside and the nightside hemispheres. This means optimal temperatures should be present on at least part of the planet, as temperature would vary with latitude. The other two exoplanets, K2-18b and LP 890-9c, have masses larger than

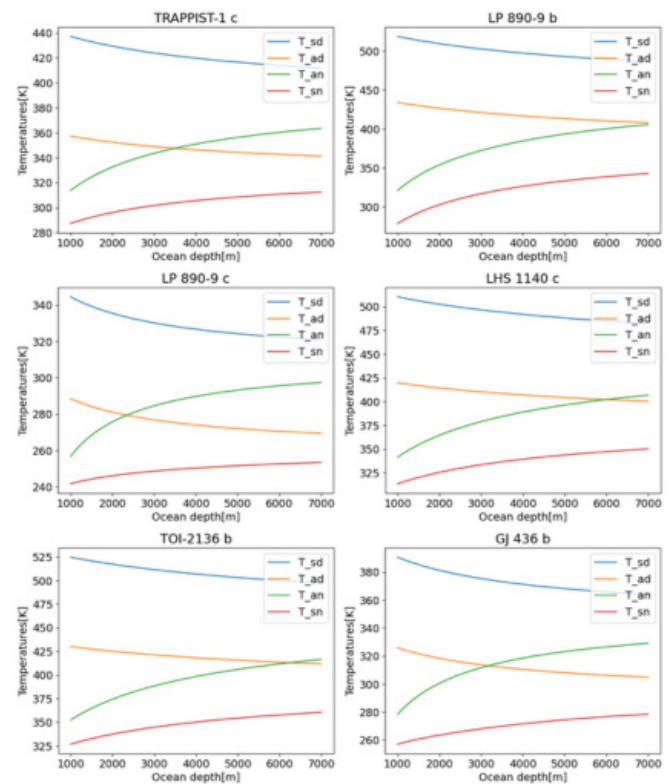


Figure 3: Temperature vs. ocean depth plots for six representative exoplanets. Surface and atmospheric temperatures calculated from our model for these tidally-locked exoplanets are plotted against ocean depth ranging from 1000–7000 meters. The plots include graphs of dayside surface temperature, T_{sd} , dayside atmospheric temperature, T_{ad} , nightside surface temperature, T_{sn} , and nightside atmospheric temperature, T_{an} .

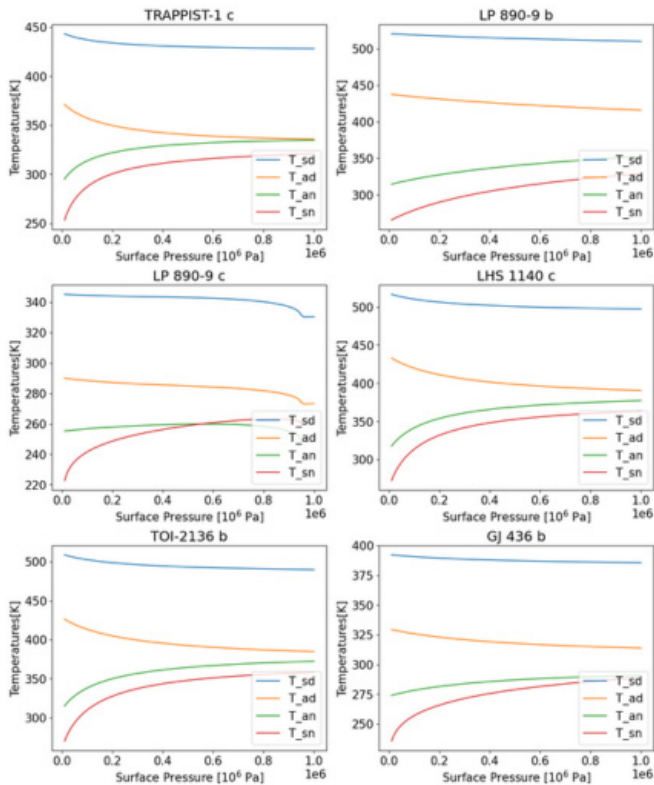


Figure 4: Temperature vs. surface pressure plots for six representative exoplanets. Surface and atmospheric temperatures calculated from our model for these tidally-locked exoplanets are plotted against the planets' surface atmospheric pressure, ranging from 104–106 Pa. The plots include graphs of dayside surface temperature, T_{sd} , dayside atmospheric temperature, T_{ad} , nightside surface temperature, T_{sn} , and nightside atmospheric temperature, T_{an} .

five times the Earth's mass, which puts them in the category of super-Earths (23, 24). The problem with these planets is that instead of having a rocky surface, they may have a "mini-Neptune" like condition, characterized by a deep atmosphere but no real surface, as has been confirmed in the case of K2-18b (23). This makes it harder for our model to predict conditions on this planet, but earlier works agree with our prediction for habitability (23). The other planet, LP 890-9c, is a newly discovered exoplanet and an important candidate for future observations, as early atmospheric characterization showing an H_2O -rich atmosphere makes the planet a favorable HZ exoplanet (24).

These climate factors are not without potential drawbacks, however, because a more dynamic ocean and atmosphere would also potentially lead to a turbulent climate. High wind speeds and larger tidal surges may accompany an effective heat transportation cycle, which can create challenging surface conditions. Our model assumes a deep atmosphere, but too much depth can lead to a runaway greenhouse effect, where atmospheric greenhouse gases block all outward thermal radiation and heat rapidly accumulates, which may put the planet beyond the question of habitability (25). While the ocean and atmospheric heat transport remain essential in order to create a habitable and moderate climate, physical parameters such as distance from the star and planetary gravitation are also key factors, for in some cases no amount

of climate factors could make the planet habitable.

One critical limitation our work faces is the dearth of exoplanetary data on specifics such as atmospheric composition and surface features. There is also a scarcity of previous works with an average prediction of these components based on the physical parameters of the planets and the planetary systems. Thus limited, we used an idealized set of parameters instead, derived from values found for the Earth (Table 1). One assumption we made was that the Earth's current ocean and atmospheric circulation dynamics would be conserved and treated it as a general condition for the exoplanets. One phenomenon that has a measurable effect on ocean and atmospheric circulation is the Coriolis Effect (26). In a tidally-locked orbit, a planet's axial orbital period becomes longer, which slows down the Coriolis effect leading the global circulation system to become more docile. Even though a dynamic system could not ideally represent a docile one, we considered dynamic circulation because HZ planets around M-type stars have shorter orbital periods, and thus such changes would not be as prominent (4, 8).

In this paper, we created an effective temperature model using the energy balance equations of tidally-locked planets. As our results showed that a uniformity in temperature lowers the possibility of extreme temperatures for tidally-locked planets, we can conclude that a larger energy distribution, and hence the presence of ocean, atmosphere, and cloud

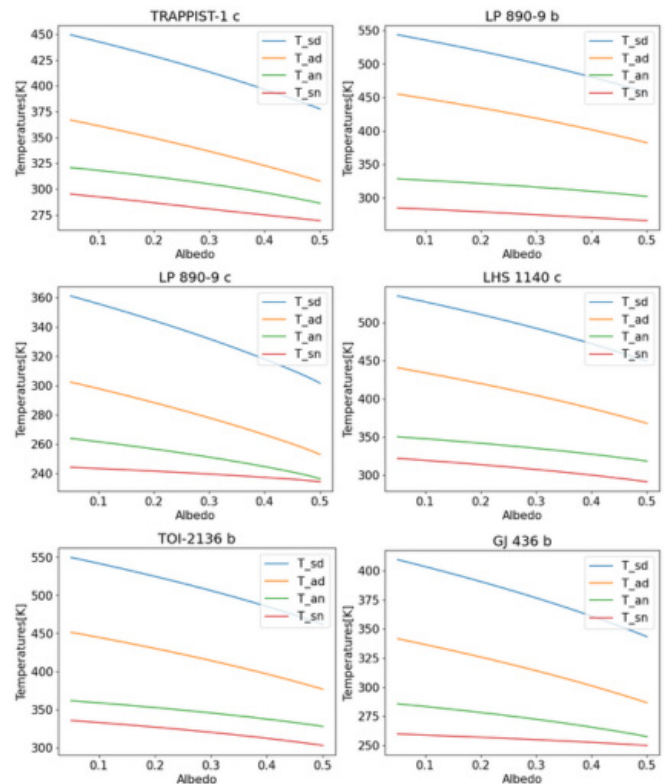


Figure 5: Temperature vs. albedo plots for six representative exoplanets. Surface and atmospheric temperatures calculated from our model for these tidally-locked exoplanets are plotted against albedo ranging from 0.05–0.5. The plots include graphs of dayside surface temperature, T_{sd} , dayside atmospheric temperature, T_{ad} , nightside surface temperature, T_{sn} , and nightside atmospheric temperature T_{an} .

coverage, would be favorable for attaining habitability. Using our model and sophisticated observational data from current and future exoplanet missions and telescopes (such as the James Webb Space Telescope), it will be possible to better determine a planet's habitability and to evaluate the role of planetary factors in achieving habitable conditions.

MATERIALS AND METHODS

Theory

Two simple box models, one each for the dayside and the nightside, were used to represent the entire planet, in which the upper half of each box represents the atmosphere and the lower half the surface (**Figure 1**) (27). The goal of our model was to solve for the dayside atmospheric and surface temperatures (T_{ad} and T_{sd} , respectively) and the nightside atmospheric and surface temperatures (T_{an} and T_{sn} , respectively) using energy balance equations of tidally-locked planets.

In the dayside, only $(1 - \alpha)$ fraction (α denotes albedo, $0 \leq \alpha \leq 1$) of the flux from the host star, S_{star} , reaches the surface, while the rest is reflected off. The dayside surface absorbs this and emits radiation at its own temperature, T_{sd} . This is partly reabsorbed by the atmosphere, which then radiates at temperature T_{ad} , half of which is absorbed by the surface. Heat fluxes, F_a and F_o , carry energy to the nightside, and the surface and atmosphere of the nightside have a relative energy transfer mechanism similar to that of the dayside. As all four systems eventually reach thermal equilibrium, the energy received exactly equals the energy going out, or $P_{in} = P_{out}$. Then, for each of the systems, the surface and atmospheric energy balance equations are,

$$\frac{S_{star}}{2} (1 - \alpha) + \epsilon_d \sigma T_{ad}^4 = \sigma T_{sd}^4 + F_o \quad (\text{Dayside surface}) \quad [\text{Eqn 1}]$$

$$\sigma T_{sd}^4 = (1 - \epsilon_d) \sigma T_{ad}^4 + 2\epsilon_d \sigma T_{ad}^4 + F_a \quad (\text{Dayside atmosphere}) \quad [\text{Eqn 2}]$$

$$F_o + \epsilon_n \sigma T_{an} = \sigma T_{sn}^4 \quad (\text{Nightside surface}) \quad [\text{Eqn 3}]$$

$$F_a + \sigma T_{sn}^4 = (1 - \epsilon_n) \sigma T_{sn}^4 + 2\epsilon_n \sigma T_{an}^4 \quad (\text{Nightside atmosphere}) \quad [\text{Eqn 4}]$$

S_{star} is the stellar flux, F_a and F_o are the atmospheric and oceanic heat transport flux, ϵ_d and ϵ_n are the emissivity for dayside and nightside atmospheres, α is the planetary albedo, and σ is the Stefan-Boltzmann constant. The derivations and calculations for these quantities follow hereafter.

The stellar constant, or stellar flux (S_{star}), can be expressed as (17),

$$S_{star} = \frac{L_{star}}{4\pi a_{pl}^2} \quad [\text{Eqn 5}]$$

Where L_{star} is the luminosity of the host star and a_{pl} is the semi-major axis of the planet. The stellar luminosity, L_{star} , is given by the Stefan-Boltzmann law (17),

$$L_{star} = 4\pi R_{star}^2 \sigma T_{effstar}^4 \quad [\text{Eqn 6}]$$

In the above equations, F_a and F_o denote the planetary atmospheric and oceanic heat transport fluxes, respectively. To express F_a and F_o in terms of known quantities, we used a modified Stommel Model for heat transport, derived using the method of dimensional analysis (28, 29). The expressions for these quantities are,

$$F_o = C_{p,w} \cdot \rho_w \cdot z_o \cdot \gamma_o \cdot (T_{sd} - T_{sn}) \quad [\text{Eqn 7}]$$

$$F_a = \frac{C_{p,a} \cdot P_s}{g} \cdot \gamma_a \cdot (T_{ad} - T_{an}) \quad [\text{Eqn 8}]$$

The description and idealized values of z_o , γ_o , γ_a , $C_{p,a}$ and P_s are listed in Table 1. $C_{p,w}$ is the specific heat of water, equal

to 4200 Jkg⁻¹K⁻¹, and g is the gravitational constant of the relevant planet, which can be calculated using Newton's law of gravitation (8),

$$g = \frac{GM_{pl}}{R_{pl}^2} \quad [\text{Eqn 9}]$$

Next, we derived formulas for the emissivity factors of the planetary atmosphere, ϵ_d and ϵ_n . We assumed a typical gray atmosphere and defined the emissivity as the ratio of absorbed to incident energy. For a CO₂, H₂O, and N₂ based atmosphere, the emissivity is related to the relative humidity (RH) of air and its water vapor pressure (17). The vapor pressure ratio (the ratio of water vapor pressure to its saturation vapor pressure) from the Clausius-Clapeyron equation is,

$$q^* = 611 \cdot e^{\frac{L_v}{R_w} \left(\frac{1}{273} - \frac{1}{T_a} \right)} \quad [\text{Eqn 10}]$$

L_v is water's latent heat of vaporization, and R_w is the gas constant for water vapor (**Table 1**).

The water vapor mixing ratio (or the mass mixing ratio for our purposes) is defined as the ratio of the mass of water vapor to the mass of dry air in a unit volume. This quantity is related to the vapor pressure ratio (q^*) (from equation 10), and the atmospheric pressure at an altitude of z from the surface. The empirical formula for the mass mixing ratio is given by (17),

$$r = \frac{r_{wet}}{r_{dry}} = 0.622 \cdot \frac{q^*}{P_a} \cdot RH \quad [\text{Eqn 11}]$$

The atmospheric pressure, P_a , from the hydrostatic equilibrium condition for ideal gas, is (8),

$$P_a = P_s \cdot e^{-\frac{z}{H}} \quad [\text{Eqn 12}]$$

Where P_s is the surface atmospheric pressure, and H is a quantity known as the scale height,

$$H = \frac{g}{R_a T} \quad [\text{Eqn 13}]$$

Where R_a is the gas constant for the atmosphere (**Table 1**) (8).

Finally, we can express the emissivity as a function of the mass mixing ratio, and therefore temperature using a modified effective atmospheric emissivity equation (30).

$$\epsilon(T) = 1 - e^{-\frac{\kappa}{r}} \quad [\text{Eqn 14}]$$

Here r is the mass mixing ratio (equation 11), and κ is a normalizing emissivity constant (**Table 1**).

Model development and data

The ultimate objective of our planetary temperature model is to solve the energy balance system of equations to find the four unknown quantities, T_{sd} , T_{ad} , T_{sn} and T_{an} . For this we used the fsolve function in Python's SciPy package (31). To incorporate the three discussed planetary factors into our solution, we used the most relevant variable parameters for each factor. For oceanic circulation, assuming the circulation rate is independent of depth for incompressible liquids, we used ocean depth as our variable parameter, as a deeper ocean has more water and thus more internal heat to transport. In the atmosphere, on the other hand, circulation rate is more significant because of its diffuse nature, and we used atmospheric pressure as the variable parameter. Lastly, due to their high reflectivity, albedo is taken as the variable parameter for cloud quantity.

After building the structure to solve the equations, to

implement the model using actual planetary data, and to determine how each of these various parameters affects planetary conditions, we used a dataset of 29 known tidally-locked HZ planets from the NASA exoplanet archive (32). From the thousands of discovered exoplanets, based on their characteristics, we selected only the tidally-locked exoplanets that are in the HZ of M-type stars. The data points we selected for each planet are: the planetary semi-major axis (a_{pl}), radius (R_{pl}), mass (M_{pl}), the host star's effective temperature ($T_{eff,star}$), and the stellar radius (R_{star}). First, we filtered through the database to find the desirable data and then converted the data into a CSV file. We then used Python's Pandas package to load the data into our model (33). Then we used these datapoints as variables in our model and ran it to obtain surface and atmospheric temperatures for each individual planet.

ACKNOWLEDGEMENTS

This research used the NASA Exoplanet Archive, which is operated by the California Institute of Technology, under contract with the National Aeronautics and Space Administration under the Exoplanet Exploration Program.

Received: June 6, 2023

Accepted: October 10, 2023

Published: August 27, 2024

REFERENCES

1. *Exoplanet Exploration: Planets beyond Our Solar System*. Accessed 20 Feb. 2023. <https://exoplanets.nasa.gov>.
2. Ricker, George R., et al. "Transiting Exoplanet Survey Satellite." *Journal of Astronomical Telescopes, Instruments, and Systems*, vol. 1, no. 1, Oct. 2014, p. 014003, <https://doi.org/10.1117/1.jatis.1.1.014003>.
3. Tarter, Jill, et al. "A Reappraisal of The Habitability of Planets around M Dwarf Stars." *Astrobiology*, vol. 7, 03 2007, pp. 30–65, <https://doi.org/10.1089/ast.2006.0124>.
4. Kasting, James F., et al. "Habitable Zones around Main Sequence Stars." *Icarus*, vol. 101, no. 1, 1993, pp. 108–128, <https://doi.org/10.1006/icar.1993.1010>.
5. McKay, Christopher P. "Requirements and Limits for Life in the Context of Exoplanets." *Proceedings of the National Academy of Sciences*, vol. 111, no. 35, 2014, pp. 12628–12633, <https://doi.org/10.1073/pnas.1304212111>.
6. Hu, Yongyun and Yang, Jun. "Role of Ocean Heat Transport in Climates of Tidally Locked Exoplanets around M Dwarf Stars." *Proceedings of the National Academy of Sciences*, vol. 111, no. 2, 2014, pp. 629–634, <https://doi.org/10.1073/pnas.1315215111>.
7. Singal, Ashok K. "Life on a Tidally-Locked Planet." *ArXiv. Org*, 2014, <https://doi.org/10.48550/ARXIV.1405.1025>.
8. Carroll, B. W., & Ostlie, D. A. (2017). *An Introduction to Modern Astrophysics* (2nd ed.). Cambridge: Cambridge University Press.
9. Shields, Aomawa L., et al. "The Habitability of Planets Orbiting M-Dwarf Stars." *Physics Reports*, vol. 663, 2016, pp. 1–38, <https://doi.org/10.1016/j.physrep.2016.10.003>.
10. Seager, Sara. "Exoplanet Habitability." *Science (New York, N. Y.)*, vol. 340, 05 2013, pp. 577–581, <https://doi.org/10.1126/science.1232226>.
11. Meadows, Victoria S. and Barnes, Rory K. "Factors Affecting Exoplanet Habitability." *Handbook of Exoplanets*, Springer International Publishing, 2018, pp. 2771–2794, https://doi.org/10.1007/978-3-319-55333-7_57.
12. Raymond, Sean. "Forget "Earth-Like"—We'll First Find Aliens on Eyeball Planets." *Nautilus*, 2018.
13. Peixoto J P., and Oort A.H. (1992) *Physics of Climate* (Am Inst Phys, NY), 520 pp.
14. Salazar, Andrea M., et al. "The Effect of Substellar Continent Size on Ocean Dynamics of Proxima Centauri b." *The Astrophysical Journal Letters*, vol. 896, no. 1, June 2020, p. L16, <https://doi.org/10.3847/2041-8213/ab94c1>.
15. Wordsworth, Robin. "Atmospheric Heat Redistribution and Collapse on Tidally Locked Rocky Planets." *The Astrophysical Journal*, vol. 806, no. 2, June 2015, p. 180, <https://doi.org/10.1088/0004-637X/806/2/180>.
16. Yang, Jun, et al. "Stabilizing Cloud Feedback Dramatically Expands the Habitable Zone of Tidally Locked Planets." *The Astrophysical Journal Letters*, vol. 771, no. 2, June 2013, p. L45, <https://doi.org/10.1088/2041-8205/771/2/L45>.
17. Pierrehumbert, Raymond T. *Principles of Planetary Climate*. Cambridge University Press, 2010.
18. Jakob, Christian. "The representation of cloud cover in atmospheric general circulation models." January 2000, <https://doi.org/10.5282/edoc.328>.
19. Koll, Daniel D. B. and Abbot, Dorian S. "Assessing the Habitability of the TRAPPIST-1 System Using a 3D Climate Model." *The Astrophysical Journal Letters*, vol. 825, no. 99, Jul. 2016, <https://doi.org/10.3847/0004-637X/825/2/99>.
20. Kaltenecker, Lisa. "How to Characterize Habitable Worlds and Signs of Life." *Annual Review of Astronomy and Astrophysics*, vol. 55, no. 1, 2017, pp. 433–485, <https://doi.org/10.1146/annurev-astro-082214-122238>.
21. Grimm, Simon L., et al. "The Nature of the TRAPPIST-1 Exoplanets." *A&A*, vol. 613, 2018, p. A68, <https://doi.org/10.1051/0004-6361/201732233>.
22. Wolf, Eric T. "Assessing the Habitability of the TRAPPIST-1 System Using a 3D Climate Model." *The Astrophysical Journal Letters*, vol. 839, no. 1, Apr. 2017, p. L1, <https://doi.org/10.3847/2041-8213/aa693a>.
23. Madhusudhan, Nikku, et al. "The Interior and Atmosphere of the Habitable-Zone Exoplanet K2-18b." *The Astrophysical Journal Letters*, vol. 891, no. 1, Feb. 2020, p. L7, <https://doi.org/10.3847/2041-8213/ab7229>.
24. Delrez, L., et al. "Two Temperate Super-Earths Transiting a Nearby Late-Type M Dwarf." *A&A*, vol. 667, 2022, p. A59, <https://doi.org/10.1051/0004-6361/202244041>.
25. Nakajima, Shinichi, et al. "A Study on the "Runaway Greenhouse Effect" with a One-Dimensional Radiative–Convective Equilibrium Model." *Journal of Atmospheric Sciences*, vol. 49, no. 23, 1992, pp. 2256–2266, [https://doi.org/10.1175/1520-0469\(1992\)049<2256:ASOTGE>2.0.CO;2](https://doi.org/10.1175/1520-0469(1992)049<2256:ASOTGE>2.0.CO;2).
26. Beesley, David, et al. "A Laboratory Demonstration of Coriolis Effects on Wind-Driven Ocean Currents." *Oceanography*, vol. 21, 06 2008, pp. 72–76, <https://doi.org/10.5670/oceanog.2008.60>.
27. Yang, Jun and Abbot, Dorian S. "A Low-Order Model of Water Vapor, Clouds, and Thermal Emission for Tidally Locked Terrestrial Planets." *The Astrophysical Journal*, vol. 784, no. 2, Mar. 2014, p. 155, <https://doi.org/10.1088/0004-637X/784/2/155>.

- [org/10.1088/0004-637X/784/2/155](https://doi.org/10.1088/0004-637X/784/2/155).
28. Stommel, Henry. "Thermohaline Convection with Two Stable Regimes of Flow." *Tellus*, vol. 13, no. 2, Wiley Online Library, 1961, pp. 224–230.
 29. Matuszak, Aleksander. "Dimensional Analysis Can Improve Equations of the Model." *Procedia Engineering*, vol. 108, 2015, pp. 526–535, <https://doi.org/10.1016/j.proeng.2015.06.174>.
 30. Brutsaert, Wilfried. "On a Derivable Formula for Long-Wave Radiation from Clear Skies." *Water Resources Research*, vol. 11, no. 5, 1975, pp. 742–744, <https://doi.org/10.1029/WR011i005p00742>.
 31. Virtanen, Pauli, et al. SciPy 1.0: Fundamental Algorithms for Scientific Computing in Python. *Nature Methods*, 17:261–272, 2020. <https://doi.org/10.1038/s41592-019-0686-2>.
 32. NASA Exoplanet Archive. *NASA Exoplanet Science Institute*. Accessed 15 Mar. 2023. <https://exoplanetarchive.ipac.caltech.edu>.
 33. The pandas development team. pandas-dev/pandas: Pandas, January 2023. <https://doi.org/10.5281/zenodo.7549438>.

Copyright: © 2024 Alamgir and Salazar. All JEI articles are distributed under the attribution non-commercial, no derivative license (<http://creativecommons.org/licenses/by-nc-nd/4.0/>). This means that anyone is free to share, copy and distribute an unaltered article for non-commercial purposes provided the original author and source is credited.